Rheological study of transient networks with junctions of limited multiplicity. II. Sol/gel transition and rheology

Tsutomu Indei[a)]
Fukui Institute for Fundamental Chemistry, Kyoto University, Kyoto 606-8103, Japan

(Received 13 November 2006; accepted 15 May 2007; published online 9 October 2007)

Viscoelastic and thermodynamic properties of transient gels formed by telechelic associating polymers are studied on the basis of the transient network theory that considers the correlation among polymer chains via network junctions. The global information of the gel is incorporated into the theory by introducing elastically effective chains defined according to the criterion of Scanlan [J. Polym. Sci. **43**, 501 (1960)] and Case [J. Polym. Sci. **45**, 397 (1960)]. We also consider the effects of superbridges whose backbone is formed by several chains connected in series and containing several breakable junctions. The dynamic shear moduli of this system are well described in terms of the Maxwell model characterized by a single relaxation time and high-frequency plateau modulus. Near the critical concentration at the sol/gel transition, superbridges become infinitely long along the backbone, thereby leading to a short relaxation time τ for the network. It is shown that τ is proportional to the concentration deviation Δ near the gelation point. The plateau modulus G_∞ increases as the cube of Δ near the gelation point as a result of the mean-field treatment, and hence the zero-shear viscosity increases as $\eta_0 \sim G_\infty \tau \sim \Delta^4$. The present model can explain the concentration dependence of the dynamic moduli observed for aqueous solutions of telechelic poly(ethylene oxide). © *2007 American Institute of Physics*.
[DOI: 10.1063/1.2747610]

I. INTRODUCTION

Transient gels formed by associating polymers have attracted widespread interests in recent years.[1] Associating polymers are polymer chains carrying specific groups capable of forming aggregates through noncovalent bonding.[2–14] Under certain thermodynamic conditions, they form a transient gel by connecting sticky groups on polymers to each other. This transformation is thermoreversible in general. In the first paper of this series[15] (referred to as I in the following), we presented a theoretical framework to study the dynamic properties of transient gels formed by multiple junctions comprising a limited number of associative groups with the intention to understand the thermodynamic properties of the linear rheology of telechelic associating polymer systems. As a first attempt, elastically effective chains (or active chains) were defined locally according to the conventional practice, i.e., chains with both ends connected to other chains were regarded to be elastically effective irrespective of whether or not these chains were incorporated into an infinite network (gel). We could qualitatively explain the concentration dependence of the dynamic shear moduli described in terms of the Maxwell model. It was shown that (i) the plateau modulus and the zero-shear viscosity increase nonlinearly with the concentration at low concentration ranges, (ii) there exists a large fraction of pairwise junctions forming concatenated chains at low concentrations, and (iii) the fraction of pairwise junctions decreases with an increase in the concentration; consequently, the relaxation time of the network increases with the concentration. However, the treatment of concatenated chains was unsatisfactory and the sol/gel transition of the system could not be treated properly due to the local definition of active chains and a lack of global information of the network.

In this study, we consider the global information of the infinite network by making use of the criterion suggested by Scanlan[16] and Case[17] for a chain to be active. This criterion states that telechelic chains are elastically effective if both their ends are connected to junctions with at least three paths to the infinite network. We assume that elastically effective chains deform according to the macroscopic deformations applied to the gel. Static properties of transient gels have been studied by Tanaka and Ishida on the basis of this criterion.[19] Here, we consider not only primary active chains (referred to as primary bridges in this paper) but also active superchains (called superbridges) whose backbone is an aggregate of several bridges connected in series. The effects of superbridges cannot be negligible, particularly in a study of the dynamic properties of transient gels, because they reduce the relaxation time of the network due to the presence of several breakable internal junctions, as suggested by Annable *et al.*[2] We can describe the transition between the sol state and the gel state in this theoretical framework. The critical behavior of viscoelastic quantities near the sol/gel transition point is shown to be significantly affected by superbridges.

It is established that telechelic polymers self-assemble in dilute solutions to form flowerlike micelles. Pham *et al.*[6,7] indicated that the solution of flowerlike micelles resembles a colloidal dispersion of adhesive hard spheres with regard to the concentration dependence of the shear modulus. Re-

[a)]Tel.: +81-75-711-7863; Fax: +81-75-781-4757. Electronic mail: indei@fukui.kyoto-u.ac.jp

cently, Meng and Russel[14] showed that the colloidal theory describing the nonequilibrium structure of dispersions under shear explains the high-frequency plateau modulus of telechelic poly(ethylene oxide) (PEO). In this paper, we attempt to theoretically describe the linear rheology of telechelic polymers in the absence of intramolecular associations. It can be shown that experimentally observed dynamic shear moduli that are characterized by a high-frequency plateau modulus and the relaxation time (and the zero-shear viscosity) are well described in terms of this theoretical treatment. This indicates that the transient network theory is a useful tool for the study of not only rheological properties but also thermodynamic properties of transient gels when it is extended so that both the correlation among polymers and the global structure of the network are taken into consideration.

This paper is organized as follows. In Sec. II, we will review the assumptions and definitions employed in I; they are also utilized in this paper. In Sec. III, linear viscoelasticities of the transient gel will be studied within the framework of the Scanlan-Case criterion for active chains. As the first step, only primary bridges are taken into consideration in this section. The effects of superbridges will be discussed in Sec. IV. In Sec. V, linear rheology (including the effects of superbridges) will be studied. Section VI will be devoted to a summary of the study.

II. ASSUMPTIONS AND DEFINITIONS OF FUNDAMENTAL QUANTITIES

We consider a solution of n linear polymers (or primary chains) per unit volume. Functional groups capable of forming junctions through noncovalent bonding are locally embedded in both ends of the primary chain. The common assumptions employed in this paper and in I are as follows: (1) any number of functional groups are allowed to be bound together to form one junction; (2) association/dissociation reactions among functional groups occur in a stepwise fashion; (3) primary chains are Gaussian chains; (4) the Rouse relaxation time of the primary chain is much shorter than the characteristic time of the macroscopic deformation applied to the system and the lifetime of the association among functional groups; (5) the looped chain formed by a single primary chain is absent (some discussion regarding the validity of this assumption is provided in Sec. V B); and (6) the molecular weight M of the primary chain is much smaller than the entanglement molecular weight, and hence the effects of the topological interactions among chains are ignored.

The terminology used in this paper (and I) are as follows: (1) the number of functional groups forming a junction (or aggregation number), say, k, is referred to as the junction multiplicity; (2) the junction with multiplicity k is called the k-junction; (3) the primary chain whose head belongs to a k-junction and whose tail is incorporated into a k'-junction is referred to as the (k,k')-chain (for convenience, we imaginarily mark one end of each chain to identify the head and tail); (4) the primary chain whose one end, irrespective of whether it is the head or tail, is incorporated into the k-junction is called the k-chain.

As in I, we define $F_{k,k'}(\mathbf{r},t)d\mathbf{r}$ as the number of (k,k')-chains at time t per unit volume with the head-to-tail vector $\mathbf{r}\sim\mathbf{r}+d\mathbf{r}$. The total number of (k,k')-chains (per unit volume) is then given by $\nu_{k,k'}(t)=\int d\mathbf{r}F_{k,k'}(\mathbf{r},t)=\nu_{k',k}(t)$, where the two subscripts of $\nu_{k,k'}(t)$ are interchangeable because the middle chain is homogeneous. It should be noted that the total number of primary chains $n=\Sigma_{k\geqslant 1}\Sigma_{k'\geqslant 1}\nu_{k,k'}(t)$ does not depend on time. The number of k-chains is given by $\chi_k(t)=\Sigma_{k'\geqslant 1}\nu_{k,k'}(t)$, and then the number of k-junctions is expressed as $\mu_k(t)=2\chi_k(t)/k$. The number of functional groups belonging to k-junctions is $k\mu_k(t)=2\chi_k(t)$ while the total number of functional groups is $2n$, so that the probability that an arbitrary chosen functional group is in a k-junction can be expressed as $q_k(t)=\chi_k(t)/n$. The above equation for the number conservation is equivalent to the normalization condition of q_k, i.e., $\Sigma_{k\geqslant 1}q_k(t)=1$. The extent of association, or the probability for a functional group to be associated with other groups, can be expressed as $\alpha(t)=\Sigma_{k\geqslant 2}q_k(t)=1-q_1(t)$.

III. THEORY ON THE BASIS OF THE SCANLAN-CASE CRITERION FOR ACTIVE CHAINS

A. Global structure of the network

Here, based on the literature,[19–21] we briefly review the manner of incorporating the global structure of the network. Under certain thermodynamic conditions, an infinite network (gel) is formed. In the postgel regime, the extent of association α' with regard to the functional groups in the sol part is different from that α'' in the gel part.[21,22] Note that $\alpha(t)$ defined in the previous section is the average extent of association for all functional groups in the system, i.e., it is expressed as

$$\alpha(t)=\alpha'(t)w_S(t)+\alpha''(t)w_G(t), \tag{1}$$

where $w_S(t)$ is the fraction of the sol part and $w_G(t)=1-w_S(t)$ is that of the gel. The sol fraction can be written as[19–21]

$$w_S(t)=\sum_{k\geqslant 1}q_k(t)\zeta_0^k, \tag{2}$$

where ζ_0 is the probability that a randomly chosen unreacted group belongs to the sol part. In the pregel regime, we have only $\zeta_0=1$. In the postgel regime, on the other hand, we have ζ_0 less than 1. Thus, ζ_0 is useful as an indicator of gelation. A primary chain belongs to the sol when both its ends are associated with the sol part, so that the sol fraction can also be expressed as

$$w_S(t)=\left(\sum_{k\geqslant 1}q_k(t)\zeta_0^{k-1}\right)^2. \tag{3}$$

Therefore, ζ_0 is a root of the following equation:

$$x=u(x), \tag{4}$$

where

$$u(x)\equiv\sum_{k\geqslant 1}q_k(t)x^{k-1}. \tag{5}$$

If Eq. (4) has more than one root, we must employ the smallest one.[19]

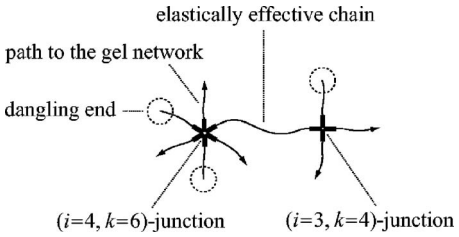

FIG. 1. A classification of the junction by the multiplicity k and the path connectivity i to the gel network. For example, a left-hand junction is formed by six functional groups but it is connected with the gel network only through four paths (represented by arrows); the other two paths are connected with dangling ends (indicated by dotted circles). A primary chain whose both ends are connected to junctions with $i \geqslant 3$ is elastically effective.

Now we consider the connectivity of a functional group to the gel network according to the theoretical treatment by Pearson and Graessley.[20] Let $\mu_{i,k}$ be the number of junctions with the multiplicity k that is connected to the gel network through i paths $(0 \leqslant i \leqslant k)$. Such a junction is called the (i,k)-junction in the following. According to the multinomial theorem, it takes the form[19,20]

$$\mu_{i,k}(t) = \mu_k(t)\frac{k!}{i!(k-i)!}\zeta_0^{k-i}(1-\zeta_0)^i. \tag{6}$$

Then, the number of paths originating from the (i,k)-junction is expressed as $\chi_{i,k}(t)=(i/2)\mu_{i,k}(t)$. Here we employ the criterion of Scanlan[16] and Case[17] to decide whether the primary chain is active. They suggested that the primary chain whose both ends are connected to junctions with a path connectivity greater than or equal to 3 is elastically effective (see Fig. 1). According to this criterion, the number of active chains whose one end belongs to k-junctions is

$$\chi_k^{\mathrm{eff}}(t) = \sum_{i\geqslant 3}^{k} \chi_{i,k}(t)$$
$$= \chi_k(t)(1-\zeta_0)[1-\zeta_0^{k-1}-(k-1)\zeta_0^{k-2}(1-\zeta_0)]. \tag{7}$$

Note that $\chi_1^{\mathrm{eff}}(t)=\chi_2^{\mathrm{eff}}(t)=0$ as it should be. The total number of active chains is then obtained as[19]

$$\nu^{\mathrm{eff}}(t) = \sum_{k\geqslant 3}\chi_k^{\mathrm{eff}}(t) = n(1-\zeta_0)^2(1-u'(\zeta_0)), \tag{8}$$

where we have used the relation $\zeta_0=u(\zeta_0)$. The number of active (k,k')-chains [i.e., the chains whose one end is connected to the (i,k)-junction with $i\geqslant 3$ and whose other end belongs to the (i',k')-junction with $i'\geqslant 3$] can be defined as

$$\nu_{k,k'}^{\mathrm{eff}}(t) = \frac{\chi_k^{\mathrm{eff}}(t)\chi_{k'}^{\mathrm{eff}}(t)}{\nu^{\mathrm{eff}}(t)}. \tag{9}$$

The following relation:

$$\sum_{k,k'\geqslant 3}\nu_{k,k'}^{\mathrm{eff}}(t) = \nu^{\mathrm{eff}}(t) \tag{10}$$

holds as it should be.

B. Time development of chains

The number of (k,k')-chains with the head-to-tail vector $\mathbf{r}$ evolves according to the following equation:

$$\frac{\partial F_{k,k'}(\mathbf{r},t)}{\partial t} + \nabla\cdot(\dot{\mathbf{r}}_{k,k'}(\mathbf{r},t)F_{k,k'}(\mathbf{r},t))$$
$$= W_{k,k'}(\mathbf{r},t) \quad (\text{for } k,k'\geqslant 3), \tag{11}$$

where $\dot{\mathbf{r}}_{k,k'}(\mathbf{r},t)$ is the rate of deformation of $\mathbf{r}$. When a macroscopic deformation is applied to the gel, only active chains deform. Some (k,k')-chains are active but the other (k,k')-chains are not because each junction has a different path connectivity even if it has the same multiplicity. To take this into account, we put

$$\dot{\mathbf{r}}_{k,k'}(t) = P_{k,k'}(t)\hat{\kappa}(t)\mathbf{r}, \tag{12}$$

where $\hat{\kappa}(t)$ is the rate of deformation tensor applied to the gel, and

$$P_{k,k'}(t) \equiv \frac{\nu_{k,k'}^{\mathrm{eff}}(t)}{\nu_{k,k'}(t)} \tag{13}$$

is the probability for a (k,k')-chain to be active. Equation (12) states that active chains deform affinely to the macroscopic deformation *on average*. Equation (11) holds for $k,k'\geqslant 3$ because both the 1 junction and 2 junction cannot have a path connectivity greater than or equal to 3 and chains connected to such junctions do not deform. These elastically ineffective primary chains are virtually in an equilibrium state; i.e., the probability distribution function that these chains take the head-to-tail vector $\mathbf{r}$ is expressed as

$$f_0(\mathbf{r}) \equiv \left(\frac{3}{2\pi Na^2}\right)^{3/2}\exp\left(-\frac{3|\mathbf{r}|^2}{2Na^2}\right), \tag{14}$$

where N and a are the number and the length of the repeat unit forming a primary chain, respectively. For example, the distribution function for the dangling chains is written as $F_{k,1}(\mathbf{r},t)=\nu_{k,1}(t)f_0(\mathbf{r})$. The right-hand side of Eq. (11) represents the net increase in the number of (k,k')-chains with the head-to-tail vector $\mathbf{r}$ per unit time due to association/dissociation reactions between end groups on the (k,k')-chain and groups on the other chains. As we have shown in I, it takes the following form:

$$W_{k,k'}(\mathbf{r},t) = -[\beta_k(r)+\beta_{k'}(r)+B_k(t)+B_{k'}(t)+P_k(t)$$
$$+P_{k'}(t)]F_{k,k'}(\mathbf{r},t)+[p_{k-1}(t)\nu_{1,k'}(t)$$
$$+p_{k'-1}(t)\nu_{k,1}(t)]f_0(\mathbf{r})+B_{k+1}(t)F_{k+1,k'}(\mathbf{r},t)$$
$$+B_{k'+1}(t)F_{k,k'+1}(\mathbf{r},t)+P_{k-1}(t)F_{k-1,k'}(\mathbf{r},t)$$
$$+P_{k'-1}(t)F_{k,k'-1}(\mathbf{r},t) \quad (\text{for } k,k'\geqslant 3), \tag{15}$$

where $\beta_k(r)$ is the probability that a functional group is dissociated from the k-junction per unit time and $p_k(t)$ is the probability for an unreacted group to be connected with the k-junction per unit time. As in I, we assume that the dissociation rate does not depend on the junction multiplicity or on the end-to-end length of the primary chain that is connected to the junction $[\beta_k(r)=\beta]$. The connection rate p_k for

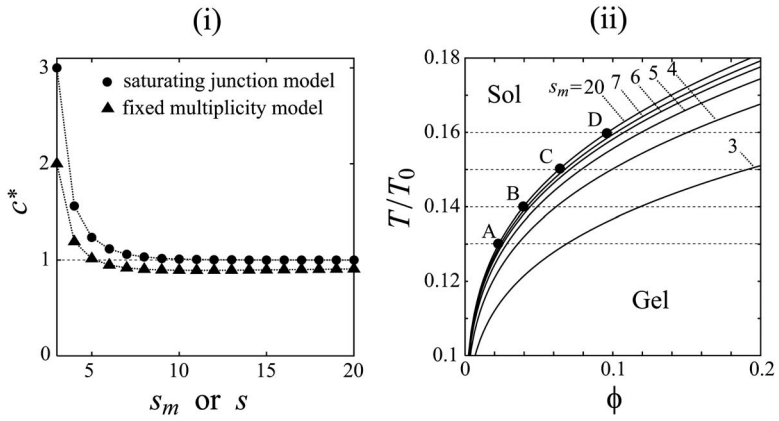

FIG. 2. (i) The reduced sol/gel transition concentration for the saturating junction model (circles) plotted against the maximum multiplicity s_m and for the fixed multiplicity model (triangles) plotted against the multiplicity s. (ii) The sol/gel transition curves drawn in the temperature-volume fraction plane for the saturating junction model with $\lambda_0=1$ and $N=100$. The maximum multiplicity varies from curve to curve. See also Fig. 9.

the connection of the functional group to a k-junction is assumed to be proportional to the volume fraction of k-junctions, and we put $p_k(t)=\beta\lambda\psi q_k(t)h_k$, where $\lambda=\exp(\epsilon/k_BT)$ is the association constant (ϵ is the binding energy for the attraction of functional groups), $\psi=2nv_0$ is the volume fraction of functional groups (v_0 is the effective volume of a segment), and h_k is a factor depending on k that provides a limit for the junction multiplicity. In the following, we use $c\equiv\lambda\psi=2\lambda\phi/N$ as the reduced polymer concentration ($\phi\equiv Nnv_0$ is the volume fraction of primary chains). Under these assumptions, $B_k(t)$ and $P_k(t)$ in Eq. (15) are given by $B_k=\beta(k-1)$ and $P_k(t)=\beta kcq_1(t)h_k$, respectively.

The kinetic equation for the (k,k')-chains has the same form as the one derived in I, i.e.,

$$\frac{d\nu_{k,k'}(t)}{dt}=w_{k,k'}(t)+w_{k',k}(t)\quad(\text{for } k,k'\geqslant 1),\tag{16}$$

where

$$w_{k,k'}(t)=-\beta k(1+cq_1(t)h_k)\nu_{k,k'}(t)+\beta k\nu_{k+1,k'}(t)+(k-1)\beta cq_1(t)h_{k-1}\nu_{k-1,k'}(t)+\beta ch_{k-1}q_{k-1}(t)\nu_{1,k'}(t)\quad(\text{for } k\geqslant 2),\tag{17a}$$

$$w_{1,k'}(t)=\beta\left(\sum_{l\geqslant 2}\nu_{l,k'}(t)+\nu_{2,k'}(t)\right)-\beta c\left(\sum_{l\geqslant 1}h_lq_l(t)+h_1q_1(t)\right)\nu_{1,k'}(t).\tag{17b}$$

Note that Eq. (11) reduces to Eq. (16) by integration with respect to $\mathbf{r}$ (for $k,k'\geqslant 3$). The kinetic equation for the k-chains also takes the same form as that derived in I. That is,

$$\frac{dq_k(t)}{dt}=\tilde{v}_k(t)\quad(\text{for } k\geqslant 1),\tag{18}$$

where

$$\tilde{v}_k(t)=-\beta k(q_k(t)-q_{k+1}(t))+\beta ck(h_{k-1}q_{k-1}(t)-h_kq_k(t))q_1(t)\quad(\text{for } k\geqslant 2),\tag{19a}$$

$$\tilde{v}_1(t)=\beta\left(\sum_{l\geqslant 2}q_l(t)+q_2(t)\right)-\beta c\left(\sum_{l\geqslant 1}h_lq_l(t)+h_1q_1(t)\right)q_1(t).\tag{19b}$$

Once $q_k(t)$ is derived by solving Eq. (18), we can obtain the number of (k,k')-chains from the relation $\nu_{k,k'}(t)=nq_k(t)q_{k'}(t)$ and ζ_0 from Eq. (4). Subsequently, $\nu^{\text{eff}}_{k,k'}(t)$ and $P_{k,k'}(t)=\nu^{\text{eff}}_{k,k'}(t)/\nu_{k,k'}(t)$ can be obtained. By substituting the expression for $P_{k,k'}(t)$ into Eq. (11) and solving the equations, $F_{k,k'}$ can be derived.

We study two special models of junctions by putting a limitation on the multiplicity, i.e., the saturating junction model and the fixed multiplicity model.[15,18,19] In the saturating junction model, we allow junctions to take only a limited range of multiplicity $k=1,2,\ldots,s_m$. This condition is realized by putting $h_k=1$ for $1\leqslant k\leqslant s_m-1$ and $h_k=0$ for $k\geqslant s_m$. In the case that $s_m=\infty$, junctions can take any value of the multiplicity without limitation. In the fixed multiplicity model, all junctions take only the same multiplicity s (except for $k=1$). This situation is approximately attained by introducing a small quantity δ ($\ll 1$) and by assuming $h_k=\delta$ for $1\leqslant k<s-1$, $h_{s-1}=\delta^{-(s-2)}$, and $h_k=0$ for $k>s-1$.[15] In most cases, δ is set to 0.01.

C. Equilibrium properties

We can obtain q_k in equilibrium by solving the equation $dq_k/dt=\tilde{v}_k=0$. It turns out to be (see I)

$$q_k=\gamma_kc^{k-1}q_1^k,\tag{20}$$

where $\gamma_k=\Pi_{l=1}^{k-1}h_l$ for $k\geqslant 2$ and $\gamma_1=1$. The fraction of unreacted groups q_1 is determined from the normalization condition $\gamma(z)q_1=1$, where $\gamma(z)\equiv\Sigma_{k\geqslant 1}\gamma_kz^{k-1}$ and $z\equiv cq_1$. The function defined by Eq. (5) can be expressed as $u(x)=\gamma(zx)/\gamma(z)$ in the equilibrium state, and hence ζ_0 is a solution of the following equation for a given z (or c):

$$x=\frac{\gamma(xz)}{\gamma(z)}.\tag{21}$$

In the case that the junction can take any value of multiplicity without limitation, for example, z is smaller than 1

(see I), and hence, $\gamma(z)=1/(1-z)$ (we can put $h_k=1$ for all k in this case). Therefore, ζ_0 is obtained as the smallest root of the equation $x=(1-z)/(1-xz)$, i.e.,

$$\zeta_0 = \begin{cases} 1 & (0 \leqslant z < z^*) \\ 1/z - 1 & (z^* < z \leqslant 1), \end{cases} \tag{22}$$

where $z^*=1/2$. Note that z^* is interpreted as the critical value of the parameter z for the sol/gel transition. The number of elastically effective chains given by Eq. (8) is then analytically expressed as a function of z,

$$\nu^{\text{eff}} = \begin{cases} 0 & (0 \leqslant z < z^*) \\ n(2(z-z^*)/z)^3 & (z^* < z \leqslant 1). \end{cases} \tag{23}$$

We can also express these quantities as a function of c by the use of the relation $z=c/(1+c)$, that is,

$$\zeta_0 = \begin{cases} 1 & (c < c^*) \\ 1/c & (c > c^*), \end{cases} \tag{24}$$

and

$$\nu^{\text{eff}} = \begin{cases} 0 & (c < c^*) \\ n((c-c^*)/c)^3 & (c > c^*), \end{cases} \tag{25}$$

where $c^*=1$ is a critical reduced concentration for gelation [see also Fig. 2(i)]. Near the sol/gel transition point, the number of elastically effective chains increases as the cube of the concentration deviation,[19] i.e., $\nu^{\text{eff}} \simeq \Delta^3$, where $\Delta \equiv (c-c^*)/c^*$. In the high concentration limit, on the other hand, all primary chains become elastically effective, i.e., $\nu^{\text{eff}} \to n$ for $c \to \infty$.

In general, the sol/gel transition point is obtained as the point at which ζ_0 becomes smaller than 1. This is equivalent to the point at which the weight-average molecular weight of the cluster diverges. For polycondensation by multiple reaction, Fukui and Yamabe[26] have shown that this condition (an appearance of a macroscopic cluster) is given by

$$(f_w - 1)(\mu_w - 1) = 1, \tag{26}$$

where f_w (=2 for the present model) is the weight-average functionality of the primary chain, and μ_w is the weight-average multiplicity of the junctions given by

$$\mu_w \equiv \sum_{k \geqslant 1} k q_k = 1 + \frac{z\gamma'(z)}{\gamma(z)}. \tag{27}$$

A boundary curve separating the sol region and gel region in the temperature-concentration plane can be drawn by the use of the equation $2\lambda(T^*)\phi^*/N=c^*$, where T^* and ϕ^* are the critical temperature and the critical volume fraction of primary chains, respectively, and c^* is obtained according to the procedure described above. The binding free energy is comprised of the energy part ϵ_0 and the entropy part S_0, so that the association constant is rewritten as $\lambda(T)=\lambda_0 \exp(T_0/T)$ with $\lambda_0 \equiv \exp(-S_0/k_B)$ and $T_0 \equiv \epsilon_0/k_B$. Thus, the critical temperature is expressed as a function of the critical volume fraction as

$$T^* = T_0/\log(Nc^*/2\lambda_0\phi^*). \tag{28}$$

Figure 2(ii) shows the sol/gel boundary lines derived from Eq. (28) for the saturating junction model.

D. Dynamic-mechanical and viscoelastic properties

We now apply a small oscillatory shear deformation with an amplitude $\tilde{\epsilon}$ to the present network. An xy component of the rate of deformation tensor is represented by $\kappa_{xy}(t) = \tilde{\epsilon}\omega \cos \omega t$ while the other components are 0 (ω is the frequency of the oscillation). Let us expand $F_{k,k'}(\mathbf{r},t)$ with respect to the powers of $\tilde{\epsilon}$ up to the first order,

$$F_{k,k'}(\mathbf{r},t) = F^{(0)}_{k,k'}(\mathbf{r}) + \tilde{\epsilon} F^{(1)}_{k,k'}(\mathbf{r},t). \tag{29}$$

Each order term takes the form (see I)

$$F^{(0)}_{k,k'}(\mathbf{r}) = \nu_{k,k'} f_0(\mathbf{r}), \tag{30a}$$

$$F^{(1)}_{k,k'}(\mathbf{r},t) = (g'_{k,k'}(\omega)\sin \omega t + g''_{k,k'}(\omega)\cos \omega t)\frac{3xy}{Na^2} f_0(\mathbf{r}). \tag{30b}$$

The number of (k,k')-chains does not depend on time as far as the small shear deformation is concerned,[23–25] so that $\nu_{k,k'}(t)$ and $q_k(t)$ can be represented by their equilibrium values $\nu_{k,k'}$ and q_k, respectively. Then, the probability for a (k,k')-chain to be elastically effective is given by its equilibrium value $P_{k,k'}=\nu^{\text{eff}}_{k,k'}/\nu_{k,k'}$ with

$$\nu^{\text{eff}}_{k,k'} = \nu_{k,k'} \frac{[1-\zeta_0^{k-1}-(k-1)\zeta_0^{k-2}(1-\zeta_0)][1-\zeta_0^{k'-1}-(k'-1)\zeta_0^{k'-2}(1-\zeta_0)]}{1-z\gamma'(\zeta_0 z)/\gamma(z)}. \tag{31}$$

The in-phase, $g'_{k,k'}(\omega)$, and out-of-phase, $g''_{k,k'}(\omega)$, amplitudes of $F^{(1)}_{k,k'}$ are directly related with the storage and loss moduli of (k,k')-chains through the relations $G'_{k,k'}(\omega)=k_BTg'_{k,k'}(\omega)$ and $G''_{k,k'}(\omega)=k_BTg''_{k,k'}(\omega)$. Because the middle chain is homogeneous, their two subscripts are exchangeable, i.e., $g'^{(n)}_{k,k'}=g'^{(n)}_{k,k'}$. Note that $g'^{(n)}_{k,1}=g'^{(n)}_{k,2}=0$ for $k \geqslant 1$ because the 2-chains and 1-chains are effectively in the equilibrium state.

Substituting Eq. (29) with Eq. (30) into Eq. (11), we obtain a set of equations for $g'^{(n)}_{k,k'}$ as follows:

$$g'_{k,k'} = (-Q_{k,k'}g''_{k,k'} + B_{k+1}g''_{k+1,k'} + B_{k'+1}g''_{k,k'+1} + P_{k-1}g''_{k-1,k'} + P_{k'-1}g''_{k,k'-1})/\omega + \nu^{\text{eff}}_{k,k'}, \tag{32a}$$

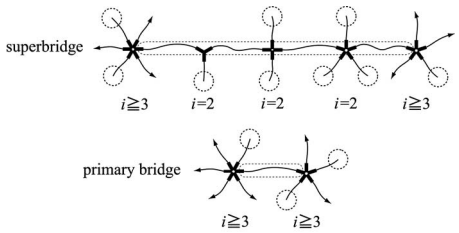

FIG. 3. Schematic representations of a superbridge (upper) and a primary bridge (lower). Bridges are surrounded by dotted curves.

$$g''_{k,k'} = (Q_{k,k'}g'_{k,k'} - B_{k+1}g'_{k+1,k'} - B_{k'+1}g'_{k,k'+1} - P_{k-1}g'_{k-1,k'} - P_{k'-1}g'_{k,k'-1})/\omega \quad (\text{for } k,k' \geqslant 3), \tag{32b}$$

where $B_k=\beta(k-1)$, $P_k=\beta kcq_1h_k$, $Q_{k,k'}(t)\equiv\beta k(1+cq_1h_k)+\beta k'(1+cq_1h_{k'})$, and $\nu^{\text{eff}}_{k,k'}$ is given by Eq. (31). It should be emphasized here that the last term in the right-hand side of Eq. (32a) is $\nu^{\text{eff}}_{k,k'}$ instead of $\nu_{k,k'}$ (see I as a reference). This is a consequence of the assumption represented by Eq. (12).

We can obtain the total moduli within the framework of the Scanlan-Case criterion for elastically effective chains by summing $G'^{(n)}_{k,k'}(\omega)$ over $k,k'\geqslant 3$, i.e.,

$$G'^{(n)}(\omega) = k_BT\sum_{k\geqslant 3}\sum_{k'\geqslant 3} g'^{(n)}_{k,k'}(\omega). \tag{33}$$

They are well described in terms of the Maxwell model with a single relaxation time (not shown here). In the high-frequency limit, Eq. (32a) reduces to $g'_{k,k'}(\omega\to\infty)=\nu^{\text{eff}}_{k,k'}$. Therefore, the plateau modulus, defined by $G_\infty\equiv G'(\omega\to\infty)$, can be expressed as

$$G_\infty = \nu^{\text{eff}}k_BT = nk_BT(1-\zeta_0)^2\left(1-\frac{z\gamma'(\zeta_0 z)}{\gamma(z)}\right). \tag{34}$$

The reduced plateau modulus $G_\infty/(nk_BT)$ coincides with the fraction of active chains derived by Tanaka and Ishida for telechelic polymers.[19] As they have shown, it agrees well with experimental data for aqueous solution of hydrophobically modified ethylene oxide-urethane copolymers (called HEUR) reported by Annable *et al.* [this also validates the assumption represented by Eq. (12)].[2] However, the relaxation time τ of the gel, determined from the peak position of $G''(\omega)$, does not agree well with experimental data, as in the case of I, because it depends on c only weakly. This discrepancy can be ascribed to the absence of *superbridges*[28] in elastically effective chains. A superbridge is a linear cluster of primary chains whose backbone includes several junctions with the path connectivity $i=2$ to the gel network. Both ends of a superbridge are connected to junctions with the path connectivity $i\geqslant 3$. Figure 3 shows an example of the superbridge whose backbone is formed by four primary chains. In the Scanlan-Case criterion, superbridges are not regarded as the elastically effective chains; only *primary bridges*, or active primary chains (see Fig. 3), are assumed to be responsible for the elasticity of the network. If we consider superbridges, not only does the number of active chains become larger but the relaxation time of the network also becomes shorter because their lifetime is shorter than that of the primary bridge due to breakable nodes within the backbone. We will discuss the effects of superbridges on $G'(\omega)$ and $G''(\omega)$ in the next section.

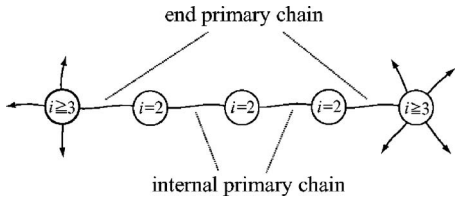

FIG. 4. Schematic of a superbridge (only paths to the network are drawn). It is comprised of two end primary chains and several internal primary chains. The number of end primary chains is $m(i\geqslant 3,i'=2)$, whereas the number of internal primary chains is $m(i=2,i'=2)$.

IV. EFFECTS OF SUPERBRIDGES

A. Number of superbridges

Let $m(i,i')$ be the number of primary chains (per unit volume) that have both their ends connected to two junctions such that the path connectivity linking one junction to the gel is i and that linking the other junction and the gel is i'. The number of primary bridges is then represented as[29]

$$m(i\geqslant 3,i'\geqslant 3) = n(1-\zeta_0)^2\left(1-\frac{z\gamma'(\zeta_0 z)}{\gamma(z)}\right) \equiv \nu^{\text{eff}}_{\text{SC}}. \tag{35}$$

The total number of primary chains incorporated into the gel through both ends is

$$m(i\geqslant 2,i'\geqslant 2) = \sum_{k\geqslant 2}\sum_{i\geqslant 2}\chi_{i,k} = n(1-\zeta_0)^2 \equiv \tilde{\nu}^{\text{eff}}, \tag{36}$$

and the number of primary chains comprising the backbones of superbridges is

$$m(i\geqslant 2,i'=2) = \sum_{k\geqslant 2}\chi_{2,k} = n(1-\zeta_0)^2\frac{z\gamma'(\zeta_0 z)}{\gamma(z)} \equiv \nu^{\text{eff}}_{\text{pseud}}. \tag{37}$$

The relation $\tilde{\nu}^{\text{eff}}=\nu^{\text{eff}}_{\text{SC}}+\nu^{\text{eff}}_{\text{pseud}}$ holds as it should be. Near the sol/gel transition concentration [or $\Delta=(c-c^*)/c^*\ll 1$], these quantities increase as $\nu^{\text{eff}}_{\text{pseud}}\sim\tilde{\nu}^{\text{eff}}\sim\Delta^2$ (and $\nu^{\text{eff}}_{\text{SC}}\sim\Delta^3$) because $1-\zeta_0$ is proportional to Δ while $z\gamma'(\zeta_0 z)/\gamma(z)$ is proportional to c. A single superbridge is comprised of two end primary chains and several internal primary chains (see Fig. 4), and therefore the relation $\nu^{\text{eff}}_{\text{pseud}}=m(i=2,i'=2)+m(i\geqslant 3,i'=2)$ must be satisfied, where

$$m(i=2,i'=2) = \sum_{k\geqslant 2}\sum_{k'\geqslant 2}\tilde{\nu}^{\text{eff}}\frac{\chi_{2,k}}{\tilde{\nu}^{\text{eff}}}\frac{\chi_{2,k'}}{\tilde{\nu}^{\text{eff}}} = \frac{(\nu^{\text{eff}}_{\text{pseud}})^2}{\tilde{\nu}^{\text{eff}}} \tag{38}$$

is the number of internal primary chains and $m(i\geqslant 3,i'=2)$ is the number of end primary chains. In Eq. (38), $\chi_{2,k}/\tilde{\nu}^{\text{eff}}$ is the probability for a chain in the network to be connected with the $(i=2,k)$-junction, and hence $\tilde{\nu}^{\text{eff}}(\chi_{2,k}/\tilde{\nu}^{\text{eff}})\times(\chi_{2,k'}/\tilde{\nu}^{\text{eff}})$ is the number of primary chains whose one end is connected with the $(i=2,k)$-junction while the other end belongs to the $(i'=2,k')$-junction. The number of superbridges is half of the number of end primary chains of superbridges, i.e.,

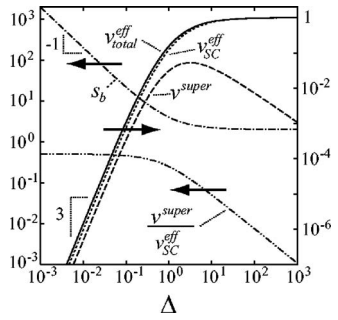

FIG. 5. The total number of elastically effective chains (solid line), the number of primary bridges or elastically effective chains defined on the basis of the Scanlan-Case criterion (dotted line), the number of superbridges (broken line), the number of primary chains per superbridge (dash-dotted line), and the ratio of the number of superbridges to that of primary bridges (dash-double dotted line) plotted against the relative concentration deviation $\Delta=(c-c^*)/c^*$ for the saturating junction model with the maximum multiplicity fixed at $s_m=15$.

$$\begin{aligned}\nu^{\mathrm{super}} &= \tfrac{1}{2}m(i\geqslant 3,i'=2)\\ &= \tfrac{1}{2}(\nu^{\mathrm{eff}}_{\mathrm{pseud}}-m(i=2,i'=2))\\ &= \frac{\nu^{\mathrm{eff}}_{\mathrm{SC}}\cdot\nu^{\mathrm{eff}}_{\mathrm{pseud}}}{2\tilde{\nu}^{\mathrm{eff}}}.\end{aligned} \tag{39}$$

Therefore, the total number of elastically effective chains turns out to be

$$\begin{aligned}\nu^{\mathrm{eff}}_{\mathrm{total}} &= \nu^{\mathrm{eff}}_{\mathrm{SC}}+\nu^{\mathrm{super}}\\ &= n(1-\zeta_0)^2\left(1-\frac{z\gamma'(\zeta_0 z)}{\gamma(z)}\right)\left(1+\frac{z\gamma'(\zeta_0 z)}{2\gamma(z)}\right).\end{aligned} \tag{40}$$

Figure 5 shows $\nu^{\mathrm{eff}}_{\mathrm{total}}$ together with the number $\nu^{\mathrm{eff}}_{\mathrm{SC}}$ of primary bridges, number ν^{super} of superbridges, and relative number of superbridges $\nu^{\mathrm{super}}/\nu^{\mathrm{eff}}_{\mathrm{SC}}$ compared to primary bridges as a function of Δ for the saturating junction model ($s_m=15$). The number of superbridges increases with the concentration near the sol/gel transition concentration ($\nu^{\mathrm{super}}\sim\Delta^3$), but it decreases at high concentrations because the number of dangling ends decreases. Thus, a peak appears in ν^{super} at modest concentrations. It should be emphasized that $\nu^{\mathrm{super}}/\nu^{\mathrm{eff}}_{\mathrm{SC}}$ increases with decreasing Δ and finally reaches 0.5, although both ν^{super} and $\nu^{\mathrm{eff}}_{\mathrm{SC}}$ become close to 0 in this limit. This indicates that the effects of superbridges cannot be ignored as compared with those of primary bridges especially in the vicinity of the sol/gel transition point. Figure 5 also shows the number of primary chains forming a superbridge defined by

$$s_b \equiv \frac{\nu^{\mathrm{eff}}_{\mathrm{pseud}}}{\nu^{\mathrm{super}}}. \tag{41}$$

With a decrease in Δ, many primary chains become incorporated into superbridges as $s_b\sim 1/\Delta$ (for $\Delta\ll 1$), indicating that the superbridge becomes longer along the backbone. With increasing concentration, on the other hand, s_b approaches 2 because $m(i=2,i'=2)$ becomes close to 0. Summarizing, in the vicinity of the sol/gel transition concentration, (i) the number of superbridges is comparable to that of primary bridges, although both are few in number, and (ii) the superbridge is infinitely long.

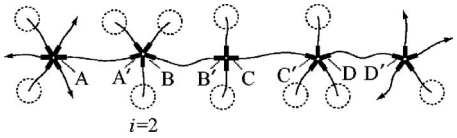

FIG. 6. An example of the superbridge whose backbone is comprised of $s_b(=4)$ primary chains.

B. Breakage rate of superbridge

Let us here focus on the primary chain whose one end is connected to the junction say, A with the path connectivity $i_{\mathrm{A}}\geqslant 3$ while the other end belongs to the junction A′ with the path connectivity $i_{\mathrm{A}'}\geqslant 2$. Such a primary chain is elastically effective.[30] In the case that $i_{\mathrm{A}'}\geqslant 3$, the chain is a primary bridge, and therefore the dissociation rate of the end group from the junction A′ is β. In the case that $i_{\mathrm{A}'}=2$, the chain is the end primary chain of the superbridge (see Fig. 6), and we assume that the breakage rate of internal chains from the junctions B,B′,C,…, is reflected in the rate at which this end primary chain is dissociated from the junction A′. Then, we can put it as the sum of its own dissociation rate β and the dissociation rate $2(s_b-1)\beta$ of $2(s_b-1)$ functional groups B,B′,…, on the internal primary chains. As a result, the dissociation rate of A′ on average can be expressed as $\beta+2(s_b-1)\rho\beta\equiv\beta^{\mathrm{eff}}$, where ρ is the probability for $i_{\mathrm{A}'}$ to be 2 and is given by $\rho=m(i\geqslant 3,i'=2)/(m(i\geqslant 3,i'\geqslant 3)+m(i\geqslant 3,i'=2))=\nu^{\mathrm{eff}}_{\mathrm{pseud}}/(\tilde{\nu}^{\mathrm{eff}}+\nu^{\mathrm{eff}}_{\mathrm{pseud}})$. We replace β in Eq. (32) with β^{eff}, in the following, in order to incorporate the short lifetime of superbridges into account. It should be noted that Eq. (20) still holds after this replacement, and therefore the discussions given in Secs. III C and IV A of this paper and Sec. IV in I remain valid. When Δ is small, β^{eff} is inversely proportional to Δ because $s_b\sim 1/\Delta$ while $\rho\sim 1$ for $\Delta\ll 1$. Therefore, we see that the relaxation time τ of the gel (approximately given as the reciprocal of β^{eff}) is proportional to Δ near the sol/gel transition concentration.

Let $\tilde{P}^{\mathrm{total}}_{k,k'}$ be the probability for a (k,k')-chain to be a primary bridge or an end primary chain of a superbridge. It can be expressed as

$$\tilde{P}^{\mathrm{total}}_{k,k'} = \frac{(\nu^{\mathrm{eff}}_{\mathrm{total}})_{k,k'}}{\nu_{k,k'}}, \tag{42}$$

where

$$(\nu^{\mathrm{eff}}_{\mathrm{total}})_{k,k'} = \frac{\nu^{\mathrm{eff}}_{\mathrm{total}}}{2}\left(\frac{\chi^{\mathrm{eff}}_k}{\nu^{\mathrm{eff}}_{\mathrm{SC}}}\frac{\tilde{\chi}^{\mathrm{eff}}_{k'}}{\tilde{\nu}^{\mathrm{eff}}}+\frac{\tilde{\chi}^{\mathrm{eff}}_k}{\tilde{\nu}^{\mathrm{eff}}}\frac{\chi^{\mathrm{eff}}_{k'}}{\nu^{\mathrm{eff}}_{\mathrm{SC}}}\right) \tag{43}$$

is the number of (k,k')-chains that is the primary bridge or the end primary chain of the superbridge. [$\tilde{\chi}^{\mathrm{eff}}_k\equiv\Sigma_{i=2}^{k}\chi_{i,k}=\chi_k(1-\zeta_0)(1-\zeta_0^{k-1})$ is the number of paths ($\geqslant 2$) originating from the $k(\geqslant 2)$-junction, and hence $\tilde{\chi}^{\mathrm{eff}}_k/\tilde{\nu}^{\mathrm{eff}}$ is the probability that a k-junction satisfies the condition $i\geqslant 2$. Similarly, $\chi^{\mathrm{eff}}_k/\nu^{\mathrm{eff}}_{\mathrm{SC}}$ is the probability for a k-junction to fulfill the condition $i\geqslant 3$. Equation (43) is expressed in a symmetric form.] Equation (43) satisfies the following relation:

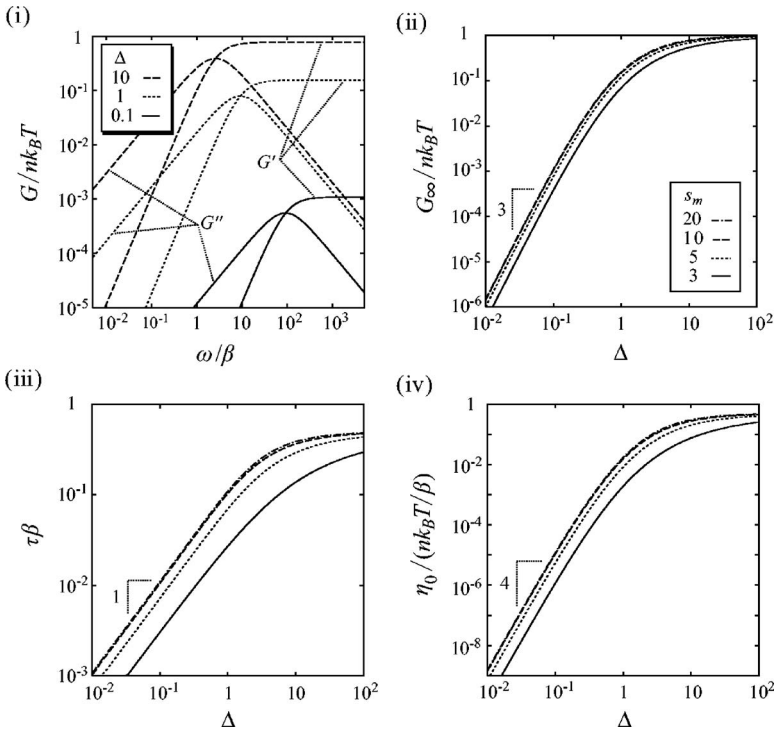

FIG. 7. (i) The reduced dynamic shear moduli for the saturating junction model as a function of the frequency. The relative concentration deviation $\Delta=(c-c^*)/c^*$ from the sol/gel transition concentration varies from curve to curve, while the maximum multiplicity of the junction is fixed at $s_m=20$. (ii) The reduced plateau modulus, (iii) relaxation time, and (iv) reduced zero-shear viscosity plotted against the relative concentration deviation for several values of the maximum multiplicity (increasing from bottom to top).

$$\sum_{k\geqslant 2}\sum_{k'\geqslant 2}(\nu_{\text{total}}^{\text{eff}})_{k,k'}=\nu_{\text{total}}^{\text{eff}} \tag{44}$$

as it should be.[31] If a macroscopic deformation is applied to the gel, not only primary bridges but also superbridges deform accordingly. According to Eq. (12), we assume that the rate of deformation vector of the (k,k')-chain is given by

$$\dot{\mathbf{r}}_{k,k'}(t)=\tilde{P}_{k,k'}^{\text{total}}\hat{\kappa}(t)\mathbf{r}. \tag{45}$$

Substituting Eq. (45) into Eq. (11), we obtain a set of equations for $g_{k,k'}^{\prime(n)}$ as given by Eq. (32) with $\nu_{k,k'}^{\text{eff}}$ replaced by $(\nu_{\text{total}}^{\text{eff}})_{k,k'}$. Therefore, in the high frequency limit, $g_{k,k'}^{\prime}$ reduces to $(\nu_{\text{total}}^{\text{eff}})_{k,k'}$. The total (observable) modulus is given by

$$G^{\prime(n)}(\omega)=k_BT\sum_{k\geqslant 2}\sum_{k'\geqslant 2}g_{k,k'}^{\prime(n)}(\omega), \tag{46}$$

and then the plateau modulus is found to be $G_\infty=G'(\omega\to\infty)=k_BT\nu_{\text{total}}^{\text{eff}}$.

V. RESULTS AND DISCUSSIONS

A. Saturating junction model

Figure 7(i) shows the dynamic shear moduli for the saturating junction model calculated from Eq. (46) (the summation is taken over $2\leqslant k, k'\leqslant s_m$). The relative concentration deviation varies from curve to curve. They are well described in terms of the Maxwell model with a single relaxation time. Near the sol/gel transition concentration ($\Delta\ll 1$), the plateau modulus and the relaxation time increase as $G_\infty\sim\Delta^3$ [see Fig. 7(ii)] and $\tau\sim\Delta$ [Fig. 7(iii)], respectively. As a result, the zero shear viscosity increases as $\eta_0\sim G_\infty\tau\sim\Delta^4$ [Fig. 7(iv)]. It is worth noting that these powers stem from the mean-field treatment.[32] For example, we can explain $\tau\sim\Delta$ as follows. Let ξ be the radius of gyration of the superbridge. Assuming that the superbridge obeys the Gaussian statistics, we have a following power law: $\xi\sim s_b^{1/2}$ for $s_b\gg 1$. Because ξ corresponds to the network mesh size, it also obeys a scaling law of the form $\xi\sim\Delta^{-\nu}$ for $\Delta\ll 1$ with $\nu=1/2$. Comparing the two expressions, we have the relation $s_b\sim 1/\Delta$. As a result, the mean lifetime of bridges (primary bridges and superbridges) that corresponds to the relaxation time of the network is approximately estimated to be $\tau\sim 1/[\beta+2(s_b-1)\rho\beta]\sim\Delta/\beta$. Figure 8 shows the dynamic shear moduli as a function of the maximum multiplicity s_m. The relaxation time increases with s_m because the number of superbridges decreases as s_m increases.

The reduced plateau modulus explicitly depends only on the reduced polymer concentration and the maximum multiplicity of the junction. Therefore, it is written as

$$\frac{G_\infty}{nk_BT}=f_1(c,s_m). \tag{47}$$

where f_1 is a dimensionless function of c and s_m. Similarly, the relaxation time and the reduced zero-shear viscosity can be expressed as

$$\beta\tau=f_2(c,s_m) \tag{48}$$

and

$$\frac{\beta\eta_0}{nk_BT}=f_3(c,s_m), \tag{49}$$

respectively (f_2 and f_3 are dimensionless functions of c and s_m). In order to investigate how the dynamic shear moduli depend on the temperature and the polymer volume fraction, let us rewrite Eqs. (47)–(49) as

$$\frac{v_0G_\infty}{k_BT_0}=\frac{\phi}{N}\frac{T}{T_0}f_1(c(T/T_0,N,\phi),s_m), \tag{50}$$

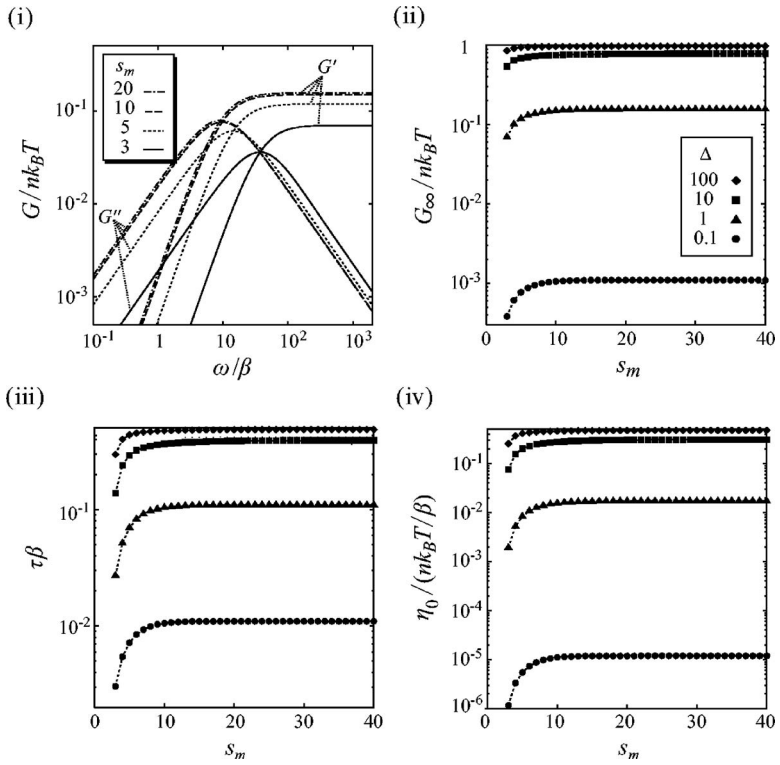

FIG. 8. (i) The reduced dynamic shear moduli for the saturating junction model as a function of the frequency. The maximum multiplicity s_m varies from curve to curve, while the relative concentration deviation is fixed at $\Delta=1$. (ii) The reduced plateau modulus, (iii) relaxation time, and (iv) reduced zero-shear viscosity plotted against the maximum multiplicity for several values of the relative concentration deviation (increasing from bottom to top).

$$\beta_0\tau = e^{T_0/T-1} f_2(c(T/T_0,N,\phi),s_m), \tag{51}$$

$$\frac{v_0\beta_0\eta_0}{k_BT_0} = \frac{\phi}{N}\frac{T}{T_0} e^{T_0/T-1} f_3(c(T/T_0,N,\phi),s_m), \tag{52}$$

respectively. We have put $W=\epsilon$ for simplicity in the derivation of Eqs. (51) and (52). In this case, the dissociation rate at temperature T is written as

$$\beta = \omega_0 e^{-\epsilon/k_BT} = \beta_0 e^{1-T_0/T}, \tag{53}$$

where β_0 is the dissociation rate at $T=T_0$. Recall that the reduced concentration depends on the temperature, molecular weight, and the polymer volume fraction as $c(T/T_0,N,\phi)=2\phi\lambda_0 e^{T_0/T}/N$. Thus, for example, the zero-shear viscosity [Eq. (52)] depends on the temperature through β ($\propto e^{1-T_0/T}$), c, and a prefactor. The unitless plateau modulus [Eq. (50)], relaxation time [Eq. (51)], and zero-

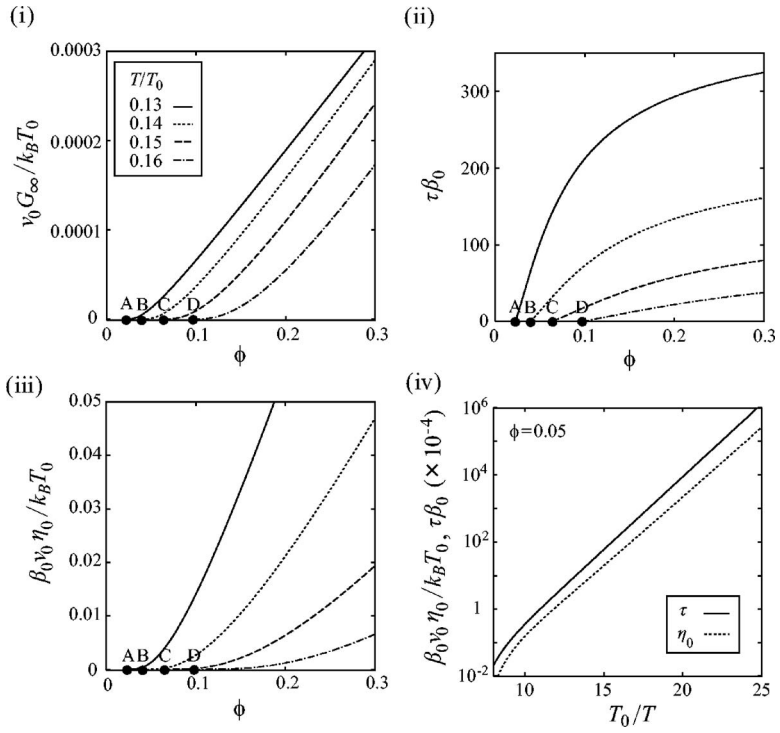

FIG. 9. (i) The plateau modulus, (ii) relaxation time, and (iii) zero-shear viscosity plotted against the polymer volume fraction for several values of the reduced temperature with $s_m=20$, $N=100$, and $\lambda_0=1$. Marked points A, B, C, and D on the horizontal axis of (i)–(iii) indicate the critical volume fraction ϕ^* for each temperature corresponding to the points in Fig. 2(ii). (iv) Arrhenius plots of the relaxation time and the zero-shear viscosity with $\phi=0.05$, $s_m=20$, $N=100$, and $\lambda_0=1$.

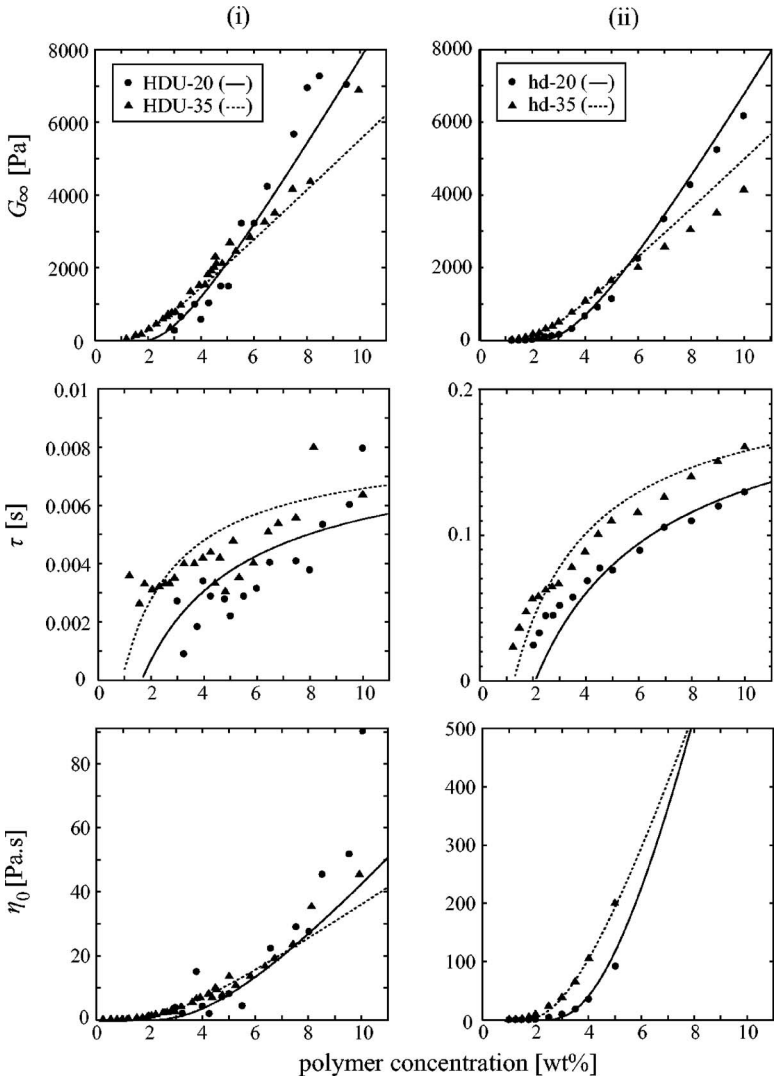

FIG. 10. Comparison between the theoretically obtained plateau modulus (top), relaxation time (middle), and zero-shear viscosity (bottom) for the saturating junction model (lines) and experimental data obtained for (i) telechelic PEO with narrow molecular weight distribution and fully end capped with C_{16} alkanes [M_w=20 kg/mol for HDU-20 (Ref. 14) and M_w=35 kg/mol for HDU-35 (Ref. 7)] and (ii) HEUR end capped with the same alkanes [M_w=20 kg/mol for hd-20 and M_w=33.1 kg/mol for hd-35 (Ref. 2)]. The values of molecular parameters s_m, β, and λv_0 used to draw theoretical curves are listed in Table I.

shear viscosity are shown in Figs. 9(i)–9(iii) as a function of the polymer volume fraction for several values of the reduced temperature T/T_0. The volume fraction ϕ varies across the sol/gel transition line drawn in Fig. 2(ii) for each temperature. When ϕ is small, G_∞ and η_0 depend on ϕ through the reduced concentration c and a prefactor, while they are approximately proportional to ϕ when ϕ (and hence c) is large because f_1 and f_3 depend only weakly on c (see Fig. 7) in this case. By contrast, τ depends on ϕ only through c. As shown in Fig. 9(iv), the zero-shear viscosity and the relaxation time approximately show the Arrhenius law temperature dependences. At higher temperature, we can see a slight deviation from the Arrhenius law. This deviation stems from the fact that τ and η_0 depend on T not only through β [see Eq. (53)] but also through c (and a prefactor in the case of η_0). At lower temperature (i.e., larger c), on the other hand, f_2 and f_3 depend only weakly on c, and therefore τ and η_0 show approximately the Arrhenius law. We can guess from Eqs. (50) and (51) that the dynamic shear moduli at temperature T can be superimposed to the curve at the reference temperature T_{ref} if they are horizontally and vertically shifted by a factor of a_T and b_T, respectively, where

$$a_T = \exp\left[-T_0\left(\frac{1}{T_{\mathrm{ref}}}-\frac{1}{T}\right)\right]\cdot\frac{f_2(c(T/T_0,N,\phi),s_m)}{f_2(c(T_{\mathrm{ref}}/T_0,N,\phi),s_m)}, \tag{54a}$$

$$b_T = \frac{T_{\mathrm{ref}}}{T}\cdot\frac{f_1(c(T_{\mathrm{ref}}/T_0,N,\phi),s_m)}{f_1(c(T/T_0,N,\phi),s_m)}. \tag{54b}$$

In particular, for large ϕ or small T, f_1 and f_2 are almost constant and independent of c; hence, Eq. (54) is approximately written as

$$a_T \simeq \exp\left[-T_0\left(\frac{1}{T_{\mathrm{ref}}}-\frac{1}{T}\right)\right], \tag{55a}$$

$$b_T \simeq \frac{T_{\mathrm{ref}}}{T}. \tag{55b}$$

It has been revealed by Annable *et al.* that the shift factor given by Eq. (55) produces the master curve successfully.[2]

In Fig. 10(i), the theoretically obtained dynamic shear moduli (i.e., plateau modulus, relaxation time, and zero-shear viscosity) for the saturating junction model are compared with the experimental data for aqueous solutions of telechelic PEO of 20 kg/mol (Ref. 14) and 35 kg/mol (Ref.

TABLE I. Values of molecular parameters used in Fig. 10.

Polymer	s_m	β (1/s)	λv_0 (nm^3)
HDU-20	20	60	1000
HDU-35	20	60	3200
hd-20	20	2.3	800
hd-35	20	2.3	2300

7) with narrow molecular weight distribution and fully end capped with C_{16} alkanes. We call these polymers HDU-20(35) according to Ref. 14. The reduced concentration c was converted into the polymer concentration in weight percentage c_w through the relation $c=(2000N_A/M)\lambda v_0 c_w$ (N_A is Avogadro's number). We have three molecular parameters for a given molecular weight: s_m, λv_0, and β. (Note that β is not required to calculate G_∞.) The values of these parameters used to draw theoretical curves are listed in Table I. We find better agreements between theory and experiment than in the case that the short lifetime of superbridges is not taken into consideration.[15] The value of λv_0 increases with the molecular weight. This indicates that the effective volume v_0 of a functional group (or a repeat unit of the chain[33]) increases with the chain length. In Fig. 10(ii), we attempt to fit theoretical curves to experimental data reported by Annable *et al.*[2] for HEUR of the similar molecular weight (but with broader molecular weight distribution) and end capped with C_{16} alkanes. They are called hd-20(35) after Ref. 14. The parameter values adopted to fit experimental data are also listed in Table I. We still find a good agreement between theory and experiment in spite of a broader molecular weight distribution of hd polymers. The difference between the values of λv_0 for HDU and hd for each (averaged) molecular weight might stem from a difference in the polydispersity of the PEO backbone. The ratio between the values of λv_0 for HDU-20 and HDU-35 (3.2) is close to that for hd-20 and hd-35 (2.9). A discrepancy between the values of β for HDU and hd might stem from the difference in the coupling agents between the alkanes and the PEO backbone, as suggested in Refs. 7 and 14.

B. Fixed multiplicity model

Figure 11 shows the dynamic shear moduli for the fixed multiplicity model together with the plateau modulus, relaxation time, and zero-shear viscosity plotted against the relative concentration deviation. These quantities obey the same critical behavior as in the saturating junction model, i.e., they increase as $G_\infty \sim \Delta^3$, $\tau \sim \Delta$, and $\eta_0 \sim \Delta^4$ near the sol/gel transition concentration.

In Fig. 12, theoretical curves are compared with experimental data for telechelic PEO. The values of parameters used to draw theoretical curves are listed in Table II. We find disagreement between theory and experiment with regard to the relaxation time; the theoretical curves increase more rapidly with the concentration as compared to experimental data, and they become roughly flat above certain concentrations. This is because the fraction of junctions with the path connectivity $i=2$ (or, in other words, the fraction of superbridges) is small in the case that the junction can possess only a single multiplicity. This tendency becomes more pronounced with an increase in the multiplicity because the fraction of $i=2$ junctions is small for a large multiplicity. Thus, we believe that the multiplicity should not be fixed at a single value. In real systems, the junctions might be cores of flowerlike micelles and the aggregation number (i.e., the number of chains per junction), say, s_{flower}, is almost independent of the polymer concentration, as some researchers have indicated. In this case, the number of bridges and dangling chains originating from a junction (i.e., multiplicity in

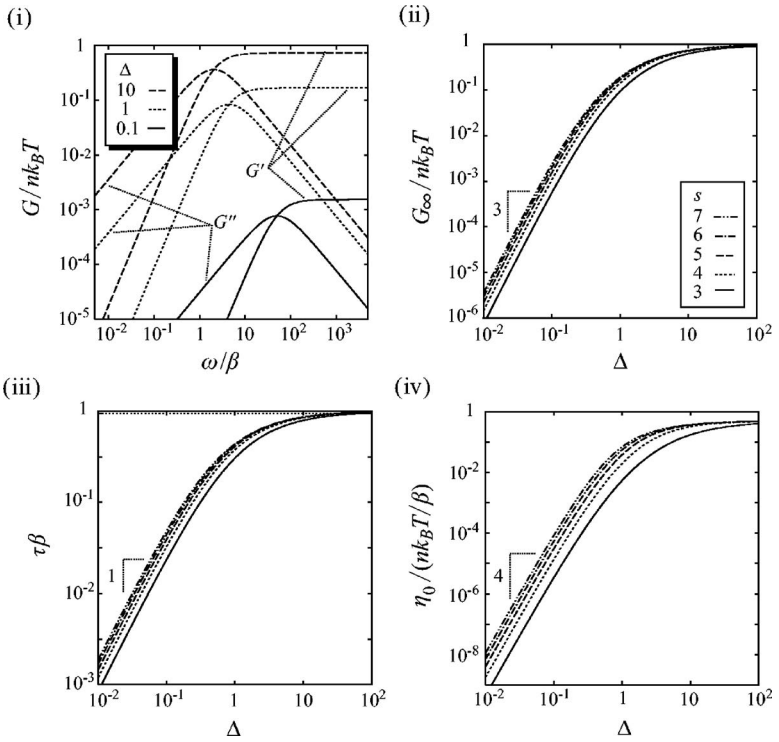

FIG. 11. (i) The reduced dynamic shear moduli for the fixed multiplicity model as a function of the frequency. The relative concentration deviation varies from curve to curve, while the multiplicity of the junction is fixed at $s=5$. (ii) The reduced plateau modulus, (iii) relaxation time, and (iv) reduced zero-shear viscosity plotted against the relative concentration deviation for several values of the junction multiplicity.

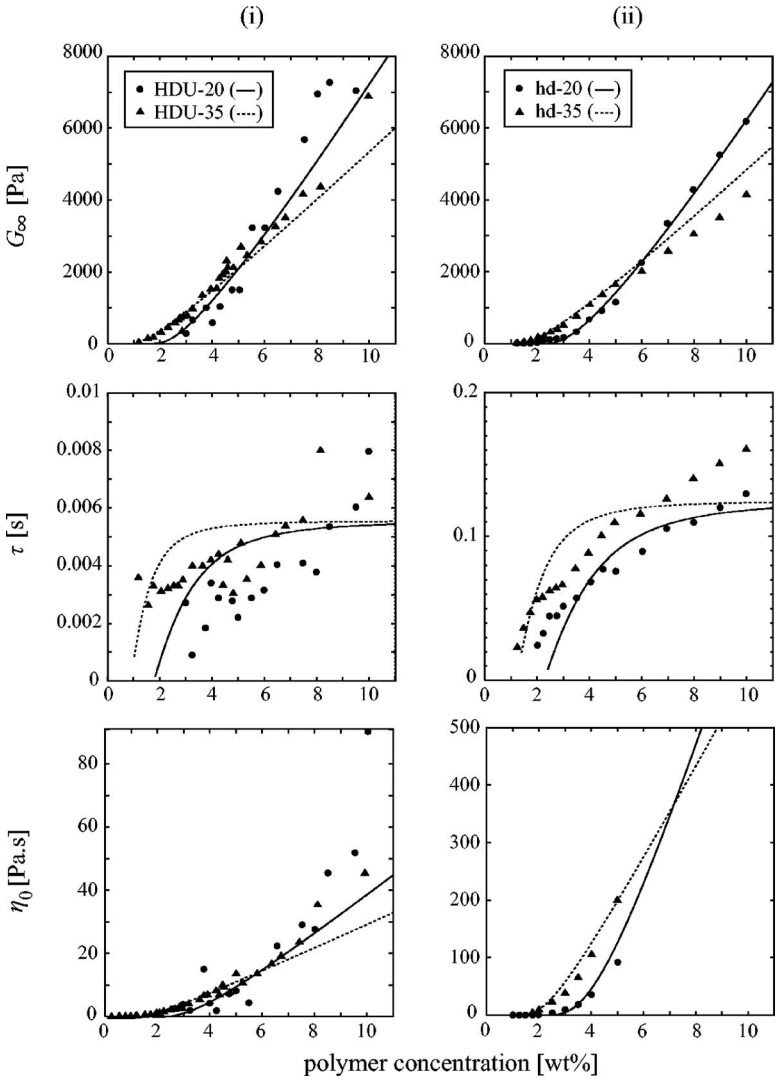

FIG. 12. Comparison between the theoretically predicted plateau modulus (top), relaxation time (middle), and zero-shear viscosity (bottom) for the fixed multiplicity model (lines) and experimental data observed for (i) telechelic PEO with narrow molecular weight distribution and fully end capped with C_{16} alkanes [M_w =20 kg/mol for HDU-20 (Ref. 14) and M_w =35 kg/mol for HDU-35 (Ref. 7)] and (ii) HEUR end capped with the same alkanes [M_w=20 kg/mol for hd-20 and M_w=33.1 kg/mol for hd-35 (Ref. 2)]. The values of molecular parameters s, β, and λv_0 used to draw theoretical curves are listed in Table II.

the present theory) can be less than s_{flower}. This situation corresponds to the saturating junction model and not the fixed multiplicity model. This might be the reason why the former model can describe the dynamic shear moduli of telechelic PEO better than the latter model.

VI. SUMMARY

We developed a theory of transient networks with junctions of limited multiplicity. The global information was incorporated into the theory by introducing the elastically effective chains (active chains) according to the criterion by Scanlan and Case and by considering the effects of superbridges whose backbone is formed by several chains connected in series. Linear viscoelasticities of the network were studied as functions of thermodynamic quantities. Near the critical concentration for the sol/gel transition, superbridges are infinitely long along the backbone and the number of superbridges is comparable to that of primary bridges. Thus, the mean lifetime of bridges is quite short near the critical point and so does the relaxation time. It was found that the relaxation time is proportional to the concentration deviation Δ near the sol/gel transition concentration. Because the plateau modulus increases as the cube of Δ as a result of the mean-field treatment, the zero-shear viscosity increases as Δ^4 near the gelation point. The dynamic shear moduli that were obtained as a function of the polymer concentration were found to agree well with the observed experimental data for aqueous solutions of telechelic PEO.

We assumed in this theoretical model that intramolecular associations (looped chains) are absent. Looped chains are thought to compete with the intermolecular association that causes bridge chains at a junction due to the limitation on the multiplicity that the junction can possess. Such competition might influence the viscoelasticity of the system. This effect and influences of additives such as surfactants and single end-capped polymers will be studied in the forthcoming paper.

TABLE II. Values of molecular parameters used in Fig. 12.

Polymer	s	β (1/s)	λv_0 (nm^3)
HDU-20	6	90	900
HDU-35	6	90	3200
hd-20	6	4	700
hd-35	6	4	2300

[1] M. A. Winnik and A. Yekta, Curr. Opin. Colloid Interface Sci. **2**, 424 (1997).
[2] T. Annable, R. Buscall, R. Ettelaie, and D. Whittlestone, J. Rheol. **37**, 695 (1993).
[3] R. D. Jenkins, D. R. Bassett, C. A. Silebi, and M. S. El-Aasser, J. Appl. Polym. Sci. **58**, 209 (1995).
[4] A. Yekta, B. Xu, J. Duhamel, H. Adiwidjaja, and M. A. Winnik, Macromolecules **28**, 956 (1995).
[5] E. Alami, M. Almgren, W. Brown, and J. Francois, Macromolecules **29**, 2229 (1996).
[6] Q. T. Pham, W. B. Russel, J. C. Thibeault, and W. Lau, Macromolecules **32**, 2996 (1999).
[7] Q. T. Pham, W. B. Russel, J. C. Thibeault, and W. Lau, Macromolecules **32**, 5139 (1999).
[8] Y. Séréro, V. Jacobsen, J.-F. Berret, and R. May, Macromolecules **33**, 1841 (2000).
[9] E. Michel, J. Appell, F. Molino, J. Kieffer, and G. Porte, J. Rheol. **45**, 1456 (2001).
[10] D. Calvet, A. Collet, M. Viguier, J.-F. Berret, and Y. Séréro, Macromolecules **36**, 449 (2003).
[11] P. Kujawa, H. Watanabe, F. Tanaka, and F. M. Winnik, Eur. Phys. J. E **17**, 129 (2005).
[12] P. Kujawa, F. Segui, S. Shaban, C. Diab, Y. Okada, F. Tanaka, and F. M. Winnik, Macromolecules **39**, 341 (2005).
[13] P. Kujawa, F. Tanaka, and F. M. Winnik, Macromolecules **39**, 3048 (2006).
[14] X.-X. Meng and W. B. Russel, J. Rheol. **50**, 189 (2006).
[15] T. Indei, J. Chem. Phys. **127**, 144904 (2007).
[16] J. Scanlan, J. Polym. Sci. **43**, 501 (1960).
[17] L. C. Case, J. Polym. Sci. **45**, 397 (1960).
[18] F. Tanaka and W. H. Stockmayer, Macromolecules **27**, 3943 (1994).
[19] F. Tanaka and M. Ishida, Macromolecules **29**, 7571 (1996).
[20] D. S. Pearson and W. W. Graessley, Macromolecules **11**, 528 (1978).
[21] P. J. Flory, *Principles of Polymer Chemistry* (Cornell University Press, Ithaca, NY, 1953), Chap. 9.
[22] W. H. Stockmayer, J. Chem. Phys. **11**, 45 (1943); **12**, 125 (1944).
[23] F. Tanaka and S. F. Edwards, Macromolecules **25**, 1516 (1992).
[24] F. Tanaka and S. F. Edwards, J. Non-Newtonian Fluid Mech. **43**, 247 (1992); **43**, 273 (1992); **43**, 289 (1992).
[25] T. Indei and F. Tanaka, J. Rheol. **48**, 641 (2004).
[26] K. Fukui and T. Yamabe, Bull. Chem. Soc. Jpn. **40**, 2052 (1967).
[27] M. Rubinstein and A. N. Semenov, Macromolecules **31**, 1386 (1998).
[28] We use the nomenclature superbridge after Ref. 2, in which a cluster formed by connecting flowerlike micelles linearly through bridges is called a superbridge. Their effects on the relaxation time are roughly estimated in this reference. In this paper, we count the number of superbridges in a more detailed way by considering the path connectivity to the network matrix to study their effects on the relaxation time.
[29] We denote the number of primary bridges as ν_{SC}^{eff} instead of ν^{eff} in the rest of this article.
[30] Internal primary chains of the superbridge are also elastically effective in the sense that they are components of the superbridge. In the present theoretical framework, however, these chains can be treated only indirectly as in the previous theory (Ref. 2). In the remaining part of this paper, the effects of these internal chains are taken into account via the end primary chains of the superbridge. For example, the breakage rate of the internal chains is reflected in the dissociation rate of the end primary chains. Furthermore, the elasticity of the superbridges is represented by that of the end primary chains by assuming that these chains deform affinely [see Eq. (45)]. This assumption is valid in the case that the macroscopic deformation applied to the gel is small, as in the present case.
[31] Note that $\chi_2^{eff}/\nu_{SC}^{eff}=0$.
[32] Rubinstein and Semenov (Ref. 27) have found the same power laws from the mean-field treatment for multifunctional polymers that can connect with each other through pairwise association between functional groups on polymers.
[33] We are assuming that both have the same effective volume.